Ion Track Formation via Electric-Field-Enhanced Energy Deposition

Zikang Ge,[1,#] Jinhao Hu,[1,#] Shengyuan Peng,[1] Wei Kang,[2] Xiaofei Shen,[3] Yanbo Xie,[4,*] and Jianming Xue[1,2,†]

[1]*State Key Laboratory of Nuclear Physics and Technology, School of Physics, Peking University, Beijing100871, China*

[2]*CAPT and HEDPS, College of Engineering, Peking University, Beijing 100871, China*

[3]*Center for Applied Physics and Technology, HEDPS, and SKLNPT, School of Physics, Peking University, Beijing 100871, China*

[4]*MOE Key Laboratory of Material Physics and Chemistry under Extraordinary Conditions, School of Physical Science and Technology, Northwestern Polytechnical University, Xian, 710072, China*

High-energy ion irradiation deposits extreme energy in a narrow range (~1-10 nm) along ion trajectories in solid through electronic energy loss, producing unique irradiation effects such as ion tracks. However, intrinsic velocity effects impose an upper limit on electronic energy loss that cannot be overcome by adjusting irradiation parameters. We introduce a method using electric fields during irradiation to enhance nanoscale energy deposition by accelerating ion-excited electrons within sub-picosecond timescales. Our extended thermal spike model quantitatively describes this enhancement and predicts a significant reduction in the electronic energy loss required for ion track formation in amorphous SiO_2, which is in excellent agreement with experimental observations. This work provides a new approach to control energy deposition during irradiation and boosts the wide application of ion tracks in material modification and nanoengineering to much broader extents.

Energetic ions penetrating solids deposit energy primarily through inelastic interactions (electronic energy loss, S_e) for high-energy irradiation, while elastic collisions (nuclear energy loss, S_n) are negligible[1,2]. This energy deposition induces rapid local heating in the solid on tens nanometer spatial scales and sub-picosecond timescales via electro-phonon coupling, followed by heat dissipation over tens to hundreds of picoseconds, forming a thermal spike that brings about various irradiation effects, such as plastic deformation[3], ionization-induced defect annealing[4,5], or even narrow trails of permanent damage along the ion path[6], called "ion track"[2,7]. These unique effects have been extensively used to characterize and modify materials, leading to broad applications in microelectronics[8], geological dating[9], biotechnology[10], and nanomaterial engineering[11].

Controlling the confined nanoscale energy deposition E_c in solids is the basis for these effects[12]. Generally, E_c equals S_e and can be modulated by varying the incident ion type and energy. However, due to intrinsic velocity effects[13], S_e values exhibit upper limits that cannot be exceeded by merely adjusting ion parameters. This imposes significant constraints on irradiation applications. For example, ion track formation remains challenging in diamond[14] and crystalline silicon[15], or even impossible in certain materials like silicon carbide[16]. Therefore, in addition to modifying ion parameters, developing an alternative method to enhance the confined energy deposition is essential.

In this Letter, we introduce a method using external electric fields during irradiation to enhance E_c, which enables ion-excited electrons to gain additional energy within sub-picoseconds. Our extended thermal spike model and multi-physics finite element simulations quantitatively describe the field-enhanced E_c

---

* Contact author: ybxie@nwpu.edu.cn
† Contact author: jmxue@pku.edu.cn

(comprising both ion-induced electronic energy loss and the field-accelerated electron energy) and subsequent thermal spike dynamics. The model reveals that field-induced electron energy synergistically evolves with electronic energy loss during sub-picosecond electron-phonon coupling, intensifying thermal spikes and promoting ion track formation—a prediction validated by our experiments. This method may open up new research areas for irradiation effects and enable innovative applications including ion-track-based nanopatterning[17,18], defect engineering[19,20], and targeted material modification at the nanoscale[21,22].

We first demonstrate through a carefully designed ion track formation experiment in amorphous SiO_2 (a-SiO_2), a key material for ion-track-based nanofabrication[2,18,23], that energy deposition is substantially enhanced when an electric field is applied during ion irradiation. Continuous ion tracks form in solids only when energy deposition exceeds a critical threshold (E_c^{th} = 4 keV/nm for a-SiO_2 [24,25]) within an extremely short timeframe (<1 ps)[21], driving local lattice atoms to melt within a nanometer-scale region (1-10 nm) along the ion trajectory. Therefore, we serve ion track formation as a criterion to determine whether energy deposition exceeds the threshold.

In our experiments, 280 nm thick a-SiO_2 thin films thermally grown on Si substrates are used as samples. These samples are divided into two experimental groups: one subjected to conventional irradiation alone, and another to our electric field enhancement method. The first group is directly irradiated in vacuum at room temperature under 2.6 MeV C ions, 4.1 MeV F ions, 6 MeV Si ions, and 20 MeV Si ions. Ion impact densities were 2×10^9 to 1×10^{10} ions/cm^2 and the angles of incidence were set to be 0° with respect to the surface normal. Under these conditions, S_e remains below the critical threshold ($S_e < S_e^{th} = E_c^{th}$=4 keV/nm, Table I), theoretically precluding ion track formation in this group. The second group experienced identical ion irradiation while simultaneously subjected to a uniform electric field of order 10^7-10^8 V/m (corresponding to applied

voltages of 10-60 V across 280 nm thick samples), provided by DC voltage and aligned with the ion incident direction, as schematically displayed in Fig. 2. Notably, as long as ion tracks form only when the external field is activated, we can conclusively establish that external fields significantly enhance energy deposition. Since ion tracks in a-SiO_2 are 'latent tracks' difficult to observe directly, the irradiated samples are etched in a 4% hydrofluoric acid (HF) aqueous solution at room temperature for 5 minutes[25] for visualization, followed by SEM characterization[26].

TABLE I. Ion irradiation parameters. The S_e and S_n are calculated by SRIM-2013 package[27]

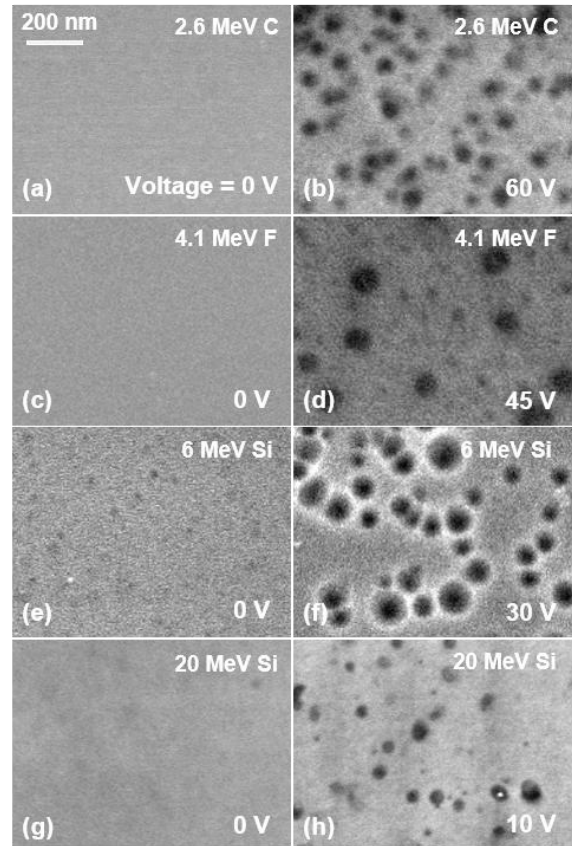| Ion	E（MeV）	S_e（keV/nm）	S_n（keV/nm）
C	2.6	1.26	0.004
F	4.1	2.01	0.009
Si	6.0	2.85	0.020
Si	20	3.48	0.007

FIG. 1 (color online). SEM images of a-SiO$_2$ films subjected to different voltage irradiated by (a)-(b) 2.6 MeV C ions, (c)-(d) 4.1 MeV F ions, (e)-(f) 6 MeV Si ions and (g)-(h) 20 MeV Si ions with 2×10^9 to 1×10^{10} ions/cm^2. The voltage applied during the irradiation is given in each image, and the electric field strength E equals the ratio of voltage to thickness 280 nm, E = voltage/280 nm.

Figure 1 compares SEM surface morphologies of a-SiO$_2$ under conventional (field-free) irradiation conditions and electric field-enhanced conditions. Figs. 1(a), (c), (e), and (g) display the etched surfaces irradiated with the traditional method; no entrance pore of ion tracks (typically appearing as round black spots in the images) can be observed on the a-SiO$_2$ surfaces. This aligns with general expectations since none of the S_e values in these cases reach the threshold S_e^{th} = 4 keV/nm required for ion track formation in a-SiO$_2$. In fact, due to the velocity effect, the maximum S_e values for C, F, and Si ions irradiation all remain below S_e^{th} regardless of the incident energy adjustments, which in principle excludes the possibility of ion track formation in a-SiO$_2$ by these three ions under any traditional irradiation conditions, shown in Supplementary Fig.S2 . However, under identical irradiation conditions, ion tracks can be formed using the electric field enhancement irradiation method. As shown in Figs. 1(b), (d), (f), and (h), entrance pores of ion tracks appear when a strong enough electric field is applied. This provides direct experimental evidence of the enhancement effect of the applied electric field on the ion track formation. Further SEM results are available in the Supplementary Fig.S3.
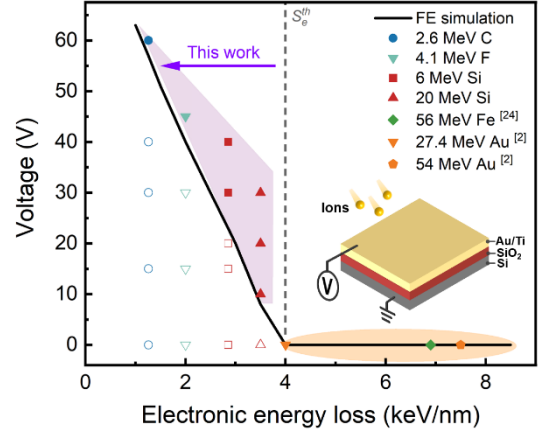

FIG. 2 (color online). Experimental results of ion track formation in a-SiO$_2$ (points) under different electronic energy loss and electric field conditions, and the new track formation criteria (black solid line) obtained from FE simulation. Solid points indicate ion track formation, while hollow points indicate no formation.

Figure 2 displays the ion track formation conditions using the electric field enhancement method (purple shaded area), which is located in the low-S_e irradiation region below the ion track formation threshold S_e^{th} of a-SiO$_2$ (shown by the vertical dashed line in the middle), also included is the high-S_e irradiation region (orange shaded area) using the traditional irradiation method. It shows that under irradiation conditions below the traditional S_e^{th}, the new method is still able to successfully form ion tracks, and the required external electric field is roughly a diagonal line in the left part, which is just the threshold energy E_c^{th}. Ion tracks cannot form in the low-E_c irradiation region (white area in the bottom left).

The rapid energy deposition in confined regions during irradiation can be described by thermal spike models These models propose that local electrons initially acquire energy from incident ions, followed by energy transfer to lattice atoms through electron-phonon coupling within an extremely short timeframe (<1 ps)[21], generating localized high-temperature thermal spikes. In conventional thermal spike models (e.g., the Analytic Thermal Spike Model, ATSM[28]), the heat source term $Q = gS_e$ derives solely from the electronic energy loss, where the electron-phonon

coupling parameter g represents the fraction of S_e contributing to lattice thermal excitation. Ion tracks form through melting-phase transitions near the ion trajectory when the irradiation-induced lattice temperature exceeds the material's melting point.
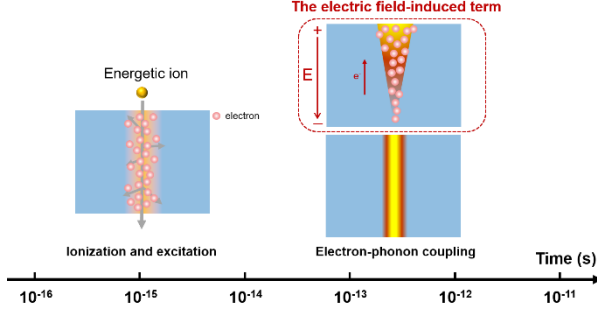

FIG. 3 (color online). Schematic diagram of the extended thermal spike dynamics process. Compared to the thermal spike model, this model adds an electric field term, making the energy deposition sources in the electron-phonon coupling process include not only electronic energy loss but also field-accelerated electron energy.

Figure 3 illustrates our extended model incorporating electric field enhancement effects. Upon initial ion incidence, electronic energy deposition induces localized ionization excitation within 10 fs, generating abundant energetic electrons. Accelerated by the strong electric field along the ion trajectory, these excited electrons gain significant field-induced kinetic energy, thereby intensifying electron-lattice collisions and amplifying the thermal spike effect. We thus extend the conventional thermal spike model by

modifying the electron-phonon coupling energy Q to an enhanced heat source Q^* that encompasses all energy transfer processes under electric field-enhanced conditions:

$$Q^* = Q(S_e) + Q(J) = gS_e + \underbrace{\iint J \cdot EdSdt}_{\text{electric field-induced term}}$$

The current density J here is governed by the carrier drift-diffusion equation is expressed as: $J(r,t) = q\mu_n nE + qD_n \nabla n$ of which spatial distribution is determined by the combined effects of the applied electric field E and electron concentration n

The localized temperature evolution under the enhanced heat source Q^* is governed by the heat conduction equation: $\rho C_p \frac{\partial T}{\partial t} = \nabla \cdot (k\nabla T) + \frac{\partial^2 Q^*}{\partial S \partial t}$. To quantitatively illustrate the subsequent effects of electric field-enhanced energy deposition, we construct a finite element model based on the extended thermal spike framework using COMSOL Multiphysics software. This model numerically reveals the thermal spike dynamics under varying bias voltages (electric field intensities) and electronic energy loss conditions, establishing critical criteria for ion track formation in SiO_2 under electric field-enhanced conditions. Following the ATSM, our simulation assumes that the irradiation electronic energy deposition takes a Gaussian distribution, and uses the melting temperature of $T_m = 2100$ K (with a phase transition latent heat of 1.14 eV/molecule[2]) as the criterion for ion track formation in a-SiO₂.
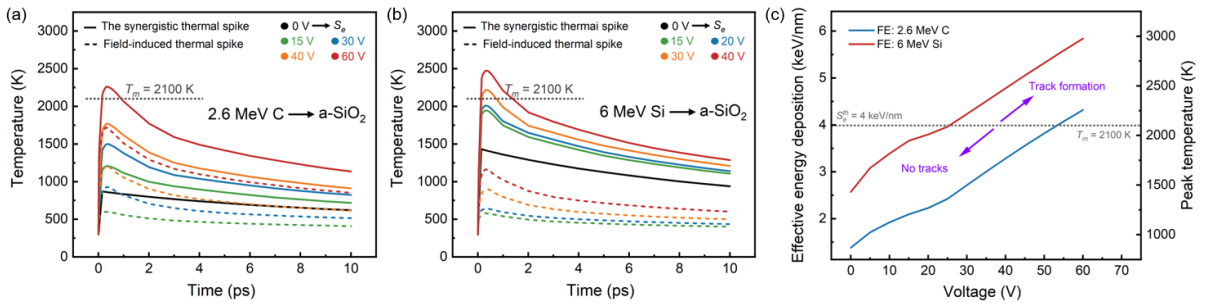

FIG. 4 (color online). Field-enhanced thermal dynamics in a-SiO₂. (a,b) Simulated temperature evolution during thermal spikes induced by 2.6 MeV C and 6 MeV Si ions, respectively. Solid lines show synergistic thermal spikes from combined ion and field effects; black solid lines represent conventional free-field cases (S_e only);

dashed lines show thermal spikes from field effects alone. (c) Effective energy deposition (left axis) and peak temperature (right axis) as functions of applied voltage. Gray dotted lines in all panels denote ion track formation thresholds. All results obtained from FE simulations incorporating our extended thermal spike model.

The synergistic evolution of thermal spikes induced by both incident ions and applied fields is key to promoting ion track formation. We performed FE simulations with varying electric field intensities under 2.6 MeV C and 6 MeV Si ion irradiation conditions to reveal this enhanced thermal spike dynamics, with results shown in Figure 4(a)(b). For the same given irradiation conditions, the contribution of ion-induced electron energy deposition (i.e., electronic energy loss, S_e) to the thermal spike remains fixed (black solid lines in Fig. 4, representing thermal spikes without electric field). While the field-induced electron energy increases with external field strength, it subsequently enhances the thermal spike effect. To determine the influence of field-induced electron energy on the synergistic thermal spike, we also simulate thermal spikes formed solely by field-induced electron energy (dashed lines in Fig. 4). Results show that field-induced thermal spike effects are comparable to or even exceed ion-induced thermal spikes. Field-accelerated electron-lattice energy transfer is complete within 0.3 ps, nearly synchronized with ion-induced thermal spike, enabling strong synergy between the two energy deposition components. Simultaneously, within such short time scale, electrons propagate only along the ion trajectory (parallel to the electric field E), with radial diffusion suppressed to a negligible level. Consequently, both energy depositions occur within the same spatial domain. This explains why the electric field enhancement method significantly enhances the confined energy deposition.

Based on their proportional contribution to thermal spikes, field-induced electron energy can be equivalently treated as an effective electronic energy loss, facilitating direct comparison with effective energy deposition E_c. When energy deposition exceeds this threshold, the local temperature of a-SiO$_2$ will simultaneously exceed the phase transition temperature, successfully forming ion tracks. Figure 4(c) illustrates how energy deposition and peak temperature vary with external electric field under 2.6 MeV C and 6 MeV Si ion irradiation, readily revealing the electric field thresholds required for ion track formation under low-S_e irradiation conditions.

The new E_c^{th} conditions for ion track formation under electric fields obtained from FE simulation are shown in Fig.2, agreeing extremely well with the experimental data in Fig. 1. With the electric field enhancement method, this threshold curve replaces the traditional irradiation S_e^{th}, revealing the pattern of electric field-enhanced energy deposition, and providing new insights for ion track formation in various solid. Semiconductor and metallic materials rarely form ion tracks under conventional irradiation, limiting their applications in fields such as nanoscale circuit patterning[29]. However, their superior electron mobility μ_n compared to a-SiO$_2$ facilitates stronger and more concentrated energy deposition in electric fields. Theoretically, semiconductors and metals could exhibit better electric field regulation effects, forming ion tracks under this new method. Additionally, the electric field enhancement method can be extended to other irradiation applications, such as ionization-induced annealing of pre-existing defects in various materials[5], offering broad applicability.

In conclusion, this work establishes a new method that applies external electric fields during irradiation to control nanoscale energy deposition, as demonstrated through track formation experiments and our extended thermal spike model. This method enhances electron-phonon coupling in the critical sub-picosecond timeframe, enabling control over effects that were previously inaccessible at given irradiation parameters. While demonstrated in a-SiO$_2$, further studies across different materials and irradiation effects will fully reveal its potential for microelectronics, materials modification, and nanostructure fabrication.

[1] M. N. Nastasi M, Mayer J, et al., *Ion-solid interactions: fundamentals and applications* Cambridge University Press, 1996).

[2] P. Kluth *et al.*, Physical Review Letters **101** (2008).

[3] S. Klaumunzer, G. Schumacher, S. Rentzsch, G. Vogl, L. Soldner, and H. Bieger, Acta Metallurgica **30**, 1493 (1982).

[4] A. Iwase, S. Sasaki, T. Iwata, and T. Nihira, Physical Review Letters **58**, 2450 (1987).

[5] Y. Zhang, R. Sachan, O. H. Pakarinen, M. F. Chisholm, P. Liu, H. Xue, and W. J. Weber, Nat Commun **6**, 8049 (2015).

[6] D. A. Young, Nature **182**, 375 (1958).

[7] M. C. Ridgway *et al.*, Physical Review Letters **110** (2013).

[8] J. R. T. a. M. Nastasi, *Handbook of Modern Ion Beam Materials Analysis* (Materials Research Society, Pittsburgh, 1995).

[9] G. A. W. a. P. V. d. Haute, *Fission-Track Dating* (Kluwer, Dordrecht, 1992).

[10] T. Kanai *et al.*, International Journal of Radiation Oncology Biology Physics **44**, 201 (1999).

[11] D. Kanjilal, Current Science **80**, 1560 (2001).

[12] R. M. Papaléo, R. Thomaz, L. I. Gutierres, V. M. de Menezes, D. Severin, C. Trautmann, D. Tramontina, E. M. Bringa, and P. L. Grande, Physical Review Letters **114** (2015).

[13] W. Assmann, M. Toulemonde, and C. Trautmann, in *Sputtering by Particle Bombardment: Experiments and Computer Calculations from Threshold to Mev Energies*, edited by R. Behrisch, and W. Eckstein2007), pp. 401.

[14] H. Amekura *et al.*, Nat Commun **15**, 1786 (2024).

[15] H. Amekura *et al.*, Sci Rep **11**, 185 (2021).

[16] J. Hanzek, S. Fazinic, S. Kumar, and M. Karlusic, Radiation Physics and Chemistry **215**, 111362 (2024).

[17] M. E. Toimil-Molares, Beilstein J Nanotechnol **3**, 860 (2012).

[18] S. Klaumunzer, Nuclear Instruments & Methods in Physics Research Section B-Beam Interactions with Materials and Atoms **225**, 136 (2004).

[19] N. Itoh, D. M. Duffy, S. Khakshouri, and A. M. Stoneham, Journal of Physics: Condensed Matter **21** (2009).

[20] R. G. Elliman and J. S. Williams, Current Opinion in Solid State and Materials Science **19**, 49 (2015).

[21] J. Zhang, M. Lang, R. C. Ewing, R. Devanathan, W. J. Weber, and M. Toulemonde, Journal of Materials Research **25**, 1344 (2011).

[22] M. Toulemonde, W. Assmann, C. Dufour, A. Meftah, and C. Trautmann, Nuclear Instruments and Methods in Physics Research Section B: Beam Interactions with Materials and Atoms **277**, 28 (2012).

[23] K. Awazu, S. Ishii, K. Shima, S. Roorda, and J. L. Brebner, Physical Review B **62**, 3689 (2000).

[24] L. A. Vlasukova, F. F. Komarov, V. N. Yuvchenko, W. Wesch, E. Wendler, A. Y. Didyk, V. A. Skuratov, and S. B. Kislitsin, Vacuum **105**, 107 (2014).

[25] A. Dallanora, T. L. Marcondes, G. G. Bermudez, P. F. P. Fichtner, C. Trautmann, M. Toulemonde, and R. M. Papaleo, Journal of Applied Physics **104**, 024307 (2008).

[26] V. E. Cosslett, Nature **323**, 212 (1986).

[27] J. P. B. J. F. Ziegler, and U. Littmark, *The Stopping and Range of Ions in Matter* (Pergamon Press, New York, 1985).

[28] G. Szenes, Nuclear Instruments and Methods in Physics Research Section B: Beam Interactions with Materials and Atoms **269**, 174 (2011).

[29] M. E. Toimil‐Molares, L. Röntzsch, W. Sigle, K. H. Heinig, C. Trautmann, and R. Neumann, Advanced Functional Materials **22**, 695 (2011).